A Subretinal Cell Delivery Method via Suprachoroidal Access in Minipigs: Safety and Surgical Outcomes

Marc D. de Smet,[1] Jessica L. Lynch,[2] Nadine S. Dejneka,[2] Michael Keane,[2] and I. John Khan[2]

[1]MicroInvasive Ocular Surgery (MIOS) Center, Lausanne, Switzerland
[2]Janssen Research & Development, LLC, Spring House, Pennsylvania, United States

Correspondence: Marc. D. de Smet, MicroInvasive Ocular Surgery (MIOS) Center, Av du Léman 32, Lausanne, 1005, Switzerland; mddesmet1@mac.com.

Submitted: May 16, 2017
Accepted: November 28, 2017

Citation: de Smet MD, Lynch JL, Dejneka NS, Keane M, Khan IJ. A subretinal cell delivery method via suprachoroidal access in minipigs: safety and surgical outcomes. *Invest Ophthalmol Vis Sci*. 2018;59:311–320. https://doi.org/10.1167/iovs.17-22233

Purpose. This study evaluated a new subretinal method for delivery of human or pig umbilical tissue–derived cells (hUTC or pUTC, respectively) using a novel subretinal injection cannula and suprachoroidal approach in Göttingen minipig eyes. hUTC (palucorcel) are currently under development for treating geographic atrophy in humans.

Methods. Twenty-four Göttingen minipigs (divided into eight groups) were subretinally administered palucorcel, pUTC, or vehicle. In some cases, fluorescently labeled cells and vehicle were administered. Conjunctival cutdown and sclerotomy were performed, then a flexible cannula containing a microneedle was inserted and advanced into the suprachoroidal space. The microneedle was deployed and visualized; 50 µL cells (target concentration, 11.2 $\times$ 10^6 cells/mL [560,000 cells/eye]) or vehicle was injected subretinally. Safety outcomes were evaluated.

Results. For all animals, cells and vehicle were successfully administered. Labeled cells or fluorescent vehicle were contained in the subretinal bleb, without leakage into the vitreous. No retinal detachment or vitreous traction band was identified by ophthalmologic examination. At all time points, observed microscopic changes were attributable to experimental procedures. On histopathology immediately after injection, localized retinal detachments were seen, along with focal retinal, choroidal, and/or scleral discontinuities. A moderate inflammatory response was seen in a limited number of animals. In the allogeneic setting, no antibody responses were detectable. Anti-human UTC antibodies were detected in the xenogeneic setting.

Conclusions. Palucorcel, pUTC, and vehicle were successfully administered to Göttingen minipigs using a novel subretinal injection cannula via a suprachoroidal surgical approach, with no significant adverse events; therefore, this technique appears to be feasible for further clinical development.

Keywords: subretinal cell delivery, suprachoroidal access, palucorcel, umbilical cells

AMD is a multifactorial, degenerative disease that is a leading cause of blindness in industrialized countries in people 55 years of age or older.[1–4] The early and intermediate stages of the disease are characterized by the accumulation of drusen and a slow loss of the choriocapillaris.[5–7] Initially, both stages are associated with minimal impairment of visual acuity.[3,8,9] However, in advanced AMD, loss of vision can be caused by either exudative neovascular ("wet") AMD or geographic atrophy (GA).[8] GA, which comprises 35% to 40% of all cases of advanced AMD, is a slowly progressive disease, characterized by loss of the RPE cells, retinal photoreceptors, and choriocapillaris, and is the cause of 20% of all cases of legal blindness in the United States.[10–11] The appearance and growth of drusen deposits are prognostic indicators for GA, and the median time to develop central GA after any GA diagnosis is 2.5 years.[12–14] The Age Related Eye Disease Study (AREDS) and Beaver Dam Eye Study demonstrated that the highest likelihood of developing GA is found in eyes with multiple large drusen (>125 µm) and in those with soft indistinct drusen, particularly when associated with macular pigmentary abnormalities.[12,14] Despite the high prevalence and burden of dry AMD, there are no therapies currently available that are effective in delaying or preventing vision loss related to GA.[15,16]

Palucorcel (CNTO 2476) is currently being evaluated as a novel cell-based therapy for the treatment of GA secondary to AMD. Palucorcel is composed of human umbilical cord tissue–derived cells (hUTC),[17] and the nature and characterization of these cells has been reported previously.[18] The cells are supplied in a proprietary cryopreserved formulation that is thawed shortly before use according to the manufacturer's instructions. Subretinal administration of palucorcel was associated with preservation of visual function in a rat model of retinal degeneration.[17] Subsequent in vitro studies showed that palucorcel was capable of rescuing RPE phagocytic dysfunction, promoting excitatory synaptic connectivity, enhancing neuronal survival, and enhancing neurite outgrowth via paracrine signaling pathways.[19,20] A recent phase 1/2a study evaluated the administration of palucorcel in 35 adults, 50 years of age and older, with bilateral GA secondary to AMD. A microcatheter delivery system (iTrack 275; iScience, Inc., Menlo Park, CA, USA) was used in conjunction with an ab externo surgical approach to access the subretinal space.[18] Palucorcel was well tolerated when delivered without retinal

perforation. There was no clinical evidence of an immune response, cell rejection, or tumor formation.[18] The low humoral immunogenicity of palucorcel observed in the phase 1/2a study was supported by previous preclinical studies showing that a single injection of pig umbilical tissue–derived cells (pUTC) in minipigs was not associated with a detectable immune response.[21,22] Although palucorcel was well tolerated in the phase 1/2a study, the ab externo surgical approach required to access the subretinal space with the microcatheter delivery system was associated with a high rate of retinal perforations (13/35 operated subjects) and retinal detachments (6/35 operated subjects).[18] In another phase 1 study in subjects with retinitis pigmentosa, inadvertent seeding into the vitreous cavity, while injecting palucorcel into the subretinal space via a transvitreal approach, was associated with retinal detachment, as well as the formation of epiretinal membranes.[23] The occurrence of retinal detachments and perforations in both early studies highlighted the need to develop a safer targeted surgical technique to deliver palucorcel into the subretinal space.

In the present study, we evaluated a novel method for the subretinal delivery of balanced salt solution (BSS+; Alcon Laboratories, Inc., Fort Worth, TX, USA), as well as both palucorcel and pUTC, using a novel subretinal injection cannula via the suprachoroidal space in minipigs. Features of this device include a flexible cannula with an advanceable microneedle for accessing the subretinal space (Fig. 1). This approach was designed to make use of the suprachoroidal space to deliver palucorcel at a specific site in the subretinal space with minimal trauma to ocular tissues while minimizing the egress of cells. The objectives of this study included the evaluation and identification of potential adverse effects associated with the use of the novel subretinal injection cannula; an assessment of the suprachoroidal surgical approach to deliver palucorcel subretinally; and the documentation of the cell injection procedure, device, and surgical performance in the preclinical setting. Additional objectives included an evaluation of the surgical healing time; characterization of postdosing disposition of administered fluorescent vehicle and carboxyfluorescein diacetate succinimidyl ester (CFSE)–labeled cells; and the identification of potential humoral immune responses as induced by the subretinal placement of either palucorcel or the pig analog, pUTC.

Methods

This study was performed in accordance with the Organization for Economic Cooperation and Development Principles of Good Laboratory Practice and as accepted by local regulatory authorities. This study was conducted at the Charles River Laboratories Montreal ULC Senneville Site (Senneville, QC, Canada). The Test Facility Quality Assurance Program monitored the study to assure the facilities, equipment, personnel, methods, practices, records, and controls conformed to Good Laboratory Practice regulations. Animal use was in adherence with the ARVO Statement for the Use of Animals in Ophthalmic and Vision Research, and the protocol was reviewed by an animal care and use committee.

Subretinal Injection Cannula

The subretinal injection cannula used in this study has a number of unique design features to improve the safety of subretinal cell delivery via a suprachoroidal approach compared to previous surgical approaches or devices used to access the subretinal space. The flexible cannula conforms to the curvature of the eye and is intended to cannulate the suprachoroidal space, reducing the risk of choroidal hemorrhage when entering the suprachoroidal space. The advanceable microneedle housed within the cannula is intended to penetrate the choroid to provide access to the subretinal space without disruption or penetration of the retina. A knob on the handle allows for controlled advancement of the microneedle, and a third arm-positioning tool is used to stabilize the cannula during insertion into the suprachoroidal space. During the surgical procedure, a BSS+ entry bleb is created prior to cell delivery. The device fluid path allows for BSS+ and cell delivery without mixing, and the BSS+ entry bleb allows for the procedure to be aborted before cells are delivered if retinal penetration is observed.

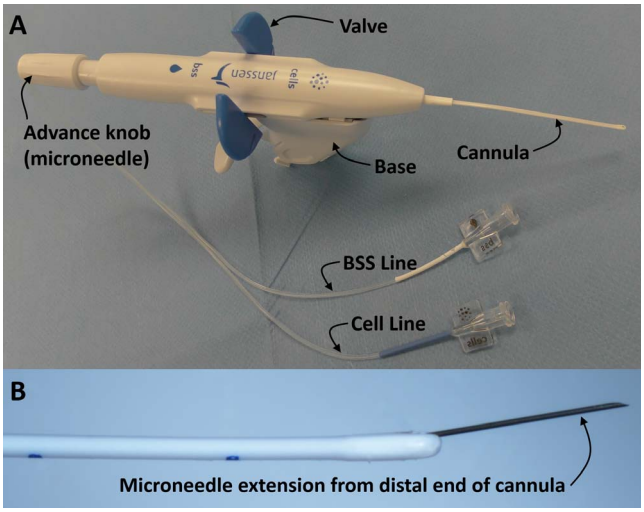

Figure 1. Picture of the subretinal injection cannula device used for cell delivery to the subretinal space of the eye.

Test Articles

Palucorcel was derived from umbilical cord tissue of a single donor as described previously.[17,18] Palucorcel was developed in compliance with all relevant regulations, including donor consent. Briefly, after digestion with enzymes, a homogenous subpopulation of umbilical cord tissue cells was isolated, cultured, and used to derive a Master Cell Bank. These cells were then prepared as a frozen suspension in CryoStor-SCO 4B/BSS (CS-SCO 4B/BSS, proprietary formulation, Janssen R&D, Spring House, PA, USA). Palucorcel was stored in liquid nitrogen vapor phase at temperatures below −120°C until ready for use.

The pUTC were isolated and expanded in a manner similar to palucorcel from pigs that were recognized by the United States Department of Agriculture as free of brucellosis, pseudorabies, transmissible gastroenteritis, and porcine reproductive and respiratory syndrome. Piglets used for deriving pUTC were vaccinated against *Mycoplasma hypopneumoniae*, *Pasteurella multocida*, *Bordetella bronchiseptica*, and *Erysipelothrix rhusiopathiae*. Adult pigs were vaccinated against *E. rhusiopathiae*, *Leptospira*, and parvovirus. Cells were formulated in 90% (vol/vol) fetal bovine serum (FBS; GE Healthcare, Logan, UT, USA) and 10% (vol/vol) dimethylsulfoxide (Sigma-Aldrich Corp., St. Louis, MO, USA) and cryopreserved in liquid nitrogen vapor phase at temperatures below −120°C.

Palucorcel and pUTC dose formulations were prepared using aseptic technique. Vials of cryopreserved cells were thawed in a water bath at 37°C. Shortly after, palucorcel was administered directly to the subretinal space. For pUTC, cells

Table 1. Dosing Groups

Group	Target Concentration, Cells/mL*		Scheduled Euthanasia
	Left Eye	Right Eye	
1	Untreated control	11.2×10^6 palucorcel labeled with CFSE†	Day 1
2	Vehicle‡ labeled with FA (1 mg/mL) and ICG (0.05 mg/mL)	11.2×10^6 pUTC labeled with CFSE†	Day 1
3	Untreated control	Vehicle‡	Month 1 (day 30)
4	Untreated control	11.2×10^6 palucorcel†	Month 1 (day 30)
5	Untreated control	11.2×10^6 pUTC†	Month 1 (day 30)
6	Untreated control	Vehicle‡	Month 3 (day 92)
7	Untreated control	11.2×10^6 palucorcel†	Month 3 (day 92)
8	Untreated control	11.2×10^6 pUTC†	Month 3 (day 92)

ICG, indocyanin green.
* All doses were administered as a single dose of 50 μL per eye.
† Target dose, 5.6×10^5 cells/eye.
‡ CS-SCO 4B/BSS.

were washed twice in BSS and resuspended in CS-SCO 4B/BSS. Cell counts were then obtained on transferred aliquots of palucorcel and pUTC to ensure that the viable cell concentrations were ≥70% in order to meet dosage level requirements for administration.

Some vials of palucorcel and pUTC were labeled with cCFSE using a kit (Vybrant CFDA SE Cell Tracker Kit; Molecular Probes, Inc., Eugene, OR, USA). Briefly, cells were thawed at 37°C in a water bath for 2 minutes. The pUTC were washed twice in BSS and resuspended in CS-SCO 4B/BSS. Palucorcel was used directly after thaw. Each cell type (330 μL) was combined with 670 μL 37°C 1X Dulbecco's phosphate buffered saline (DPBS; Life Technologies, Carlsbad, CA, USA). Cells were subsequently incubated with 0.5 μL 5 mM CFSE for 15 minutes in the dark. The reaction was quenched by adding 1 mL 37°C FBS. Cells were washed twice with 1X DPBS using centrifugation. Cellular pellets were resuspended in 10% FBS prepared in 1X DPBS such that the target concentration was 11.2×10^6 cells/mL (560,000 cells/eye).

Animals and Treatment Administration

Male Göttingen minipigs were obtained from Marshall BioResources (North Rose, NY, USA). Animals were between 9 and 10.5 months old and weighed 12.9 to 17.6 kg at the start of the study. Animals were assigned to treatment groups by a stratified randomization scheme designed to achieve similar group body weights. Animals were single-housed in stainless steel cages with an automatic watering valve and had access to a standard certified commercial laboratory diet (Harlan Teklad Miniswine Diet 8753; Harlan Laboratories, Inc., Madison, WI, USA) twice daily except during specified study procedures.

A total of 24 Göttingen minipigs were divided into eight equal treatment groups. In preparation for dose administration, a topical antibiotic (0.3% tobramycin) was applied to both eyes twice on the day before and the day after subretinal injection. Tobramycin was also applied to some eyes 2 days before dose administration. Animals were fasted overnight or for an appropriate period before the dosing procedure and anesthetized via intramuscular injection of a sedative cocktail of ketamine (22 mg/kg), glycopyrrolate (0.01 mg/kg), and acepromazine (1.1 mg/kg). An isoflurane/oxygen mix was administered to the animals via an endotracheal tube during the procedure. The conjunctivas were then flushed with benzalkonium chloride (Zephiran; Sanofi-Aventis US, LLC, Bridgewater, NJ, USA) diluted in sterile water to 1:10,000 (vol/vol). Topical anesthetic drops (proparacaine) were applied, along with tropicamide 1% and/or cyclopentolate 1% mydriatic drops (Cyclogyl; Alcon Laboratories, Inc.) to obtain suitable pupil dilation. Animals received intravenous lactated Ringer's solution (10 mL/kg/h) during the dosing procedure to aid in recovery from anesthesia.

On day 1, a single subretinal injection of vehicle (CS-SCO 4B/BSS; groups 3 and 6), palucorcel (target concentration, 11.2×10^6 cells/mL [targeted dose, 5.6×10^5 cells] in CS-SCO 4B/BSS; groups 1, 4, and 7), or pUTC (target concentration 11.2×10^6 cells/mL [targeted dose, 5.6×10^5 cells] in CS-SCO 4B/BSS; groups 2, 5, and 8) was administered in a volume of 50 μL in the right (treated) eye (Table 1). These injections were preceded by injection of a small volume of BSS+ for bleb formation. For groups 1 and 2, palucorcel and pUTC, respectively, were fluorescently labeled with CFSE before administration. Animals in group 2 received vehicle CS-SSCO 4B/BSS containing fluorescein (FA) and indocyanine green (ICG) in the left eye. For all other groups, the left eye was untreated and did not undergo surgical procedures. The dose of palucorcel used in this study was based on the highest dose used in prior clinical studies.[18] An equivalent dose of pUTC was used to facilitate comparison of potential effects in the xenogeneic and allogeneic setting.

Animals in groups 1 and 2 were terminated on the day of surgery; those in groups 3 to 5 were terminated at month 1 (day 30); and those in groups 6 to 8 were terminated at month 3 (day 92; Table 1).

Suprachoroidal Surgical Approach and Subretinal Injection Cannula

All surgeries were performed by a single vitreoretinal surgeon. The conjunctiva was opened, and the underlying sclera was freed from any overlying connective tissue. A marker was used to indicate the position of retaining sutures (6-0 Vicryl sutures; Ethicon, Inc., Somerville, NJ, USA) and the position and size of a sclerotomy, parallel but located 8 to 9 mm posteriorly to the limbus. The sclerotomy was created using a crescent knife, and the remaining scleral fibers were removed with a Sinsky hook. The diameter was adjusted to allow for passage of the cannula while providing a snug fit. The subretinal injection cannula was passed under the retaining sutures and advanced tangential to the eye through the sclerotomy, approximately 3 to 5 mm into the suprachoroidal space. Once in position, the cannula was sutured to the surface of the sclera to prevent unwanted movement of the cannula. Using indirect ophthalmoscopy to visualize the cannula tip, the microneedle was carefully advanced into the subretinal space. A small BSS+ entry bleb was created to confirm that the microneedle tip was in the subretinal space. This was followed by the administration of cells (560,000 cells/eye) or vehicle in a 50-μL volume forming a

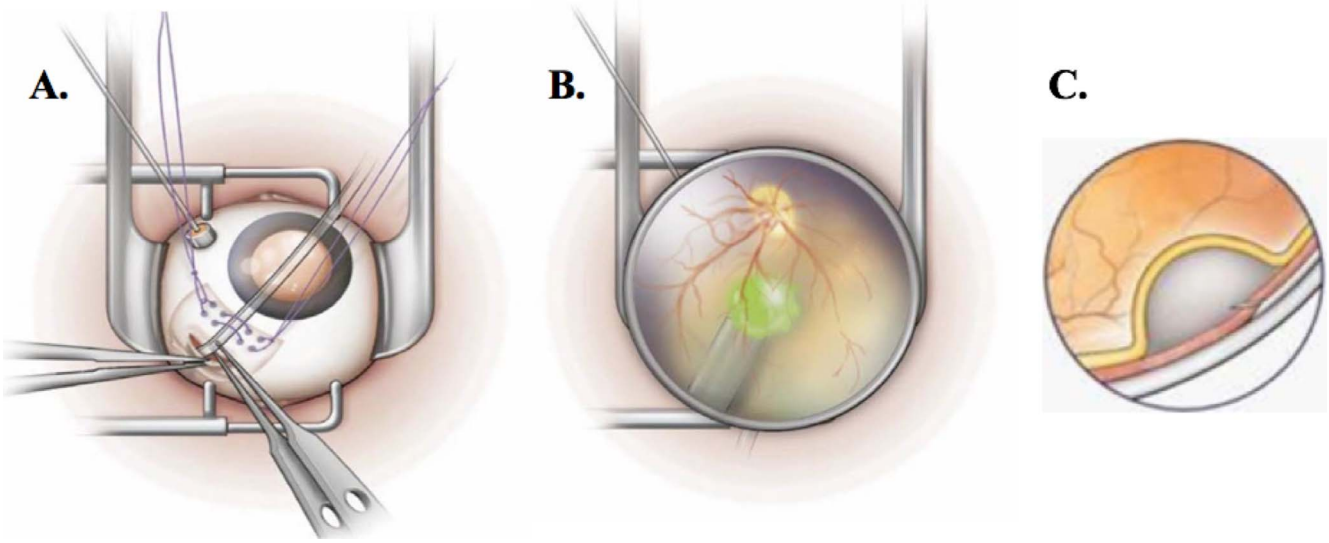

FIGURE 2. Depiction of the insertion and delivery of palucorcel to the subretinal space. (**A**) Insertion of the cannula (through suture loops) into the suprachoroidal space via a sclerotomy. (**B**) Fundus view of the cannula positioned within the suprachoroidal space (visible under the retina) with cells and vehicle being dispensed (depicted as *green*) into the subretinal space approximately two disc diameters away from the optic nerve. (**C**) Microneedle penetrating through the choroid to form a subretinal bleb.

small bleb around the microneedle tip (Fig. 2). The microneedle was then retracted, and the cannula was removed. The sclerotomy and conjunctiva were closed using Vicryl sutures.

Study Assessments

Minipigs first underwent routine ophthalmic examinations using a handheld slit lamp. Eyes were then dilated with 1% tropicamide and examined using an indirect ophthalmoscope. All ophthalmic examinations were performed by a trained ophthalmic veterinarian. FA and ICG angiography using a scanning laser ophthalmoscope (Spectralis; Heidelberg Engineering, Heidelberg, Germany) and electroretinography (ERG) (LKC UTAS-E-4000 with EMWin software) were performed at predetermined time points, as described below. In eyes that had received CFSE-labeled cells or vehicle with a fluorescent dye, fluorescence was measured using the blue filter on the Spectralis imaging system on the day of injection. Ophthalmic examinations were performed once before treatment; on days 3, 7, and 15; approximately 1 month after surgery; and monthly thereafter. Fundus imaging was performed once before and immediately following the surgical procedure on day 1 for animals who received fluorescently labeled cells or vehicle with fluorescent dye. FA and ICG angiography were performed once before treatment, at 1 month after dosing, and before necropsy. No postdose angiography was performed on animals euthanized on day 1. ERG was performed once before treatment and before necropsy for all animals except those euthanized on day 1. Following necropsy, histopathology was performed on each eye by a board-certified veterinary pathologist.

Intraoperative assessments included the device's ability to access the suprachoroidal space, the ease of insertion and advancement into this space, the microneedle's ability and ease of accessing the subretinal space, and the microneedle's ability to deliver the product. These outcomes were recorded during or directly following the procedure using a formalized questionnaire. Any complications, such as a hemorrhage in any ocular compartment, retinal perforation and/or delivery of vehicle or cells to the vitreous, leakage of injected formulation after microneedle withdrawal, or collapse of the bleb following the removal of the cannula, were also recorded. Routine monitoring and safety assessments, including body weights, food consumption, and clinical pathology parameters (hematology, coagulation, clinical chemistry) were evaluated based on clinical observations and blood samples. Serum was collected once before treatment (on all animals); during weeks 1 and 2; and at months 1, 2, and 3 (depending on scheduled euthanasia) and was tested for the presence of IgG antibodies against palucorcel or IgG antibodies against pUTC using flow cytometry.

Detection of Anti-hUTC or Anti-pUTC IgG Antibodies in Serum

Serum samples were analyzed for the detection of anti-hUTC or anti-pUTC IgG antibodies using a flow cytometry method. Briefly, hUTC or pUTC were cultured to confluence and subsequently activated by addition of 25 ng/mL human IFN-γ (Invitrogen, Carlsbad, CA, USA) or 80 ng/mL porcine IFN-γ (R&D Systems, Inc., Minneapolis, MN, USA), respectively, for 48 hours. Cells were harvested and then treated with normal minipig serum (NMS), undiluted test samples, or undiluted positive controls (porcine serum obtained from pigs immunized with pUTC or hUTC). Fluorochrome-labeled antibodies against pig IgG antibodies were used as a secondary reagent to allow detection of pig anti-pUTC or pig anti-hUTC IgG antibodies by flow cytometry. Negative controls (secondary antibody only) were used to set the flow cytometer (FACSCalibur; Beckton-Dickinson, Franklin Lakes, NJ, USA) voltages by setting the peak geometric mean fluorescence (GMF) between 10^0 and 10^1 (log histogram), while the NMS control represented background signal. A sample was considered positive if that sample's GMFSample/GMFNegative ratio was above the set cut-point. The pre- and all postdose samples from each animal were analyzed in the same experiment on IFN-γ–activated hUTC and pUTC cells. The cut-point was established to be 1.013 for anti-hUTC IgG and 0.960 for anti-pUTC IgG. Postdose samples that were found to be positive based on the cut-point were further evaluated by comparing their GMF against the GMF of their respective predose sample (GMFPostdose/GMFPredose) to see if an increase in anti-hUTC or anti-

pUTC IgG was observed during the dosing phase when compared to predose levels. A postdose sample that showed an increase greater than 30% (GMFPostdose /GMFPredose ratio > 1.3) compared to the corresponding predose sample was considered as potentially containing anti-hUTC or anti-pUTC IgG antibodies.

Terminal Procedures

Animals were subjected to a complete necropsy examination. Eyes and optic nerves were collected and preserved in Davidson's fixative. The eyelids, extraocular muscle, and nictitating membrane (bilateral) were preserved in 10% neutral buffered formalin. Tissues were embedded in paraffin, sectioned, mounted on glass slides, and stained with hematoxylin and eosin. For each eye, at least two slides were prepared for sagittal sections from each of the following locations: the sclerotomy incision site, the catheter tract, the bleb areas (if visible), and the optic nerves. Histopathological evaluation was performed by a board-certified veterinary pathologist at Charles River Labs in Montreal. Select images were captured at the discretion of the study pathologist with the Aperio Digital Image Capture System (Leica Biosystems, Buffalo Grove, IL, USA).

Results

Palucorcel Exposure and Fundus Imaging

Palucorcel, pUTC, and vehicle were successfully administered using the subretinal injection cannula and suprachoroidal surgical procedure in all animals. The targeted cell concentration of palucorcel and pUTC across all dose groups was 11.2×10^6 cells/mL (560,000 cells/eye). Actual concentrations of palucorcel delivered ranged from 7.93×10^6 to 11.98×10^6 cells/mL. Actual concentrations of pUTC delivered ranged from 6.88×10^6 to 14.68×10^6 cells/mL.

Immediately post dose, CFSE-labeled palucorcel was clearly visible as multifocal pinpoints of hyperfluorescence located in the bleb in autofluorescence fundus images (example shown in Fig. 3A). The fluorescent vehicle was clearly visible as a discrete area of hyperfluorescence in the bleb area during fundus imaging (example shown in Fig. 3B). Based on fundus imaging, no leakage of cells or vehicle into the vitreous was observed.

Surgical Observations

In all operated eyes, the procedure was performed as planned without any device failure. Cannula insertion into the suprachoroidal space was rated as very easy or easy for the majority of operated eyes (23/27). Possible retinal perforations were reported in four of 27 operated eyes, and partial bleb collapse was noted in six of 27 operated eyes. A subretinal hemorrhage was noted in one of the 27 operated eyes, but in no case did a choroidal or subretinal hemorrhage prevent successful delivery (Table 2).

Clinical Observations

As expected, there were no unscheduled deaths during the study. Following surgery, there were no clinical signs (e.g., changes in body weight, food consumption, clinical pathology parameters) that were considered related to palucorcel or pUTC. The observed clinical signs were related to the experimental procedures. Ocular clinical signs included ocular discharge, conjunctival hyperemia, and periorbital swelling, as well as periorbital skin staining and scabbing. These clinical signs generally resolved within the first month, although conjunctival hyperemia persisted through day 52 in animals euthanized at month 3. Hyperemia was not associated with any signs of intraocular inflammation.

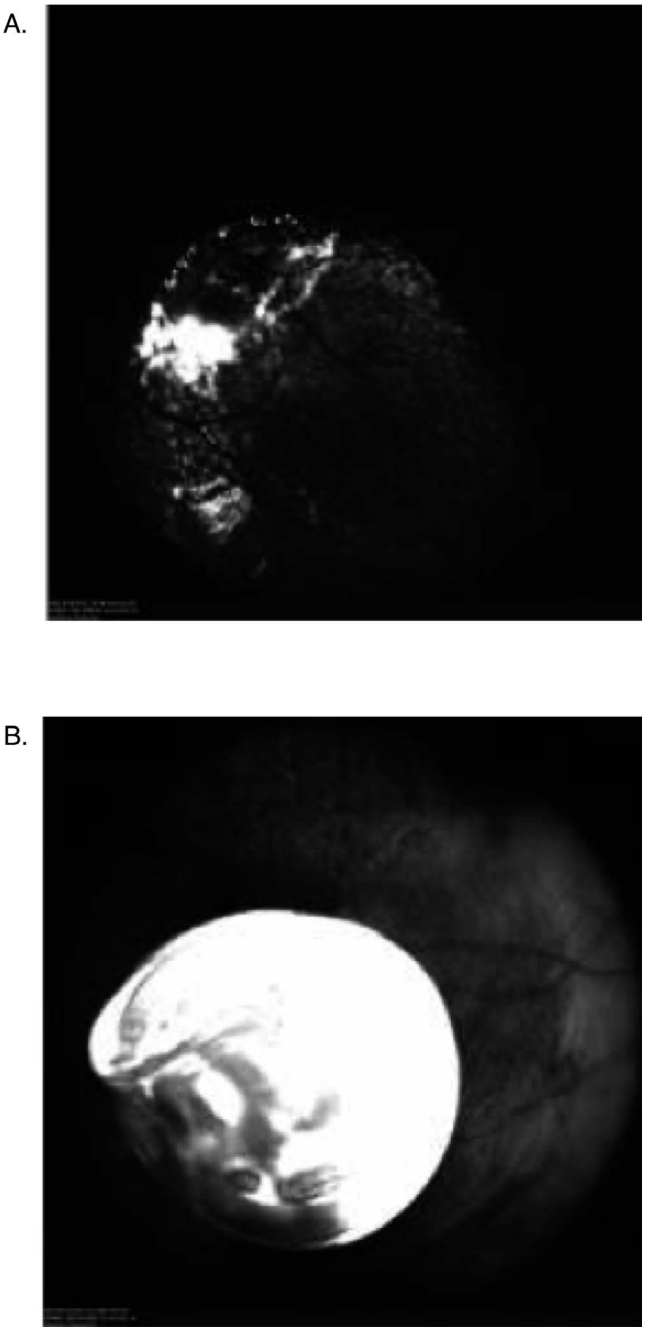

Figure 3. Autofluorescence imaging of (**A**) CFSE-labeled palucorcel within the subretinal bleb immediately post surgery and (**B**) cell vehicle containing 1 mg/mL FA and 0.05 mg/mL ICG illuminating the region of the subretinal bleb.

Ophthalmic Observations

Ophthalmic observations for eyes administered with CS-SCO vehicle, palucorcel, or pUTC are summarized in Supplementary Table S1. Diffuse hyperemia, hemorrhage, and swelling resulting from the surgery improved significantly over the first few weeks. Minor corneal findings (focal or diffuse opacities

Table 2. Summary of Intraoperative Assessment Findings

Group	Euthanized Day 1		Euthanized Month 1			Euthanized Month 3		
Intraoperative Assessment Findings, No. of Eyes Affected	Palucorcel	Vehicle/pUTC	Vehicle	Palucorcel	UTC	Vehicle	Palucorcel	pUTC
No. of eyes evaluated	3	6	3	3	3	3	3	3
Device accessed the suprachoroidal space	3	6	3	3	3	3	3	3
Cannula perforated the choroid	–	1	–	–	–	–	–	–
Microneedle accessed the subretinal space	3	6	3	3	3	3	3	3
Retinal perforation occurred	–	3	–	–	–	–	–	1
Due to microneedle	–	2	–	–	–	–	–	1
Due to cannula	–	1	–	–	–	–	–	–
Hemorrhage prevented subretinal delivery	–	–	–	–	–	–	–	–
Subretinal hemorrhage	–	–	–	–	1	–	–	–
Product was delivered to the subretinal space	3	6	3	3	3	3	3	3
Product was visible in vitreous after delivery	–	1	–	–	–	–	–	–
Bleb collapsed after device withdrawal	–	4	–	–	1	1	–	–
General device failure		–	–	–	–	–	–	–
Ease of cannula insertion into suprachoroidal space								
Very easy	2	5	3	2	3	3	3	2
Easy	–	–	–	–	–	–	–	1
Somewhat difficult	–	1	–	–	–	–	–	–
Difficult	1	–	–	1	–	–	–	–

and superficial vascularization) related to the experimental procedures improved or resolved during the initial postoperative month, although slight focal corneal opacities remained present in two eyes at 3 months post dose. Minor retinal changes (focal grayish retinal haze, irregular retina/choroid pigmentation, focal/multifocal hemorrhages, and focal retina/choroid opacities) related to the experimental procedures improved or resolved during the first postoperative month. Slight to moderate focal retinal elevations caused by bleb formation during the dosing procedure were observed at day 3 in all vehicle-treated eyes and resolved within 1 week.

Similar to vehicle, subretinal administration of palucorcel or pUTC caused minor observable changes. There was no sign of ocular inflammation. At the site of injection, the following minor alterations were observed: slight to moderate grayish cell-like retinal opacities suggestive of cellular aggregates that were present in the subretinal space of all palucorcel-treated eyes and most pUTC-treated eyes. These grayish opacities, which were not present in vehicle-treated eyes, resolved within 1 to 2 months after dosing. Slight to moderate focal retinal elevations caused by bleb formation were observed on day 3 in eyes receiving palucorcel or pUTC. These had resolved by 1 month. Similar focal retinal elevations were observed in vehicle-treated eyes, but resolved more rapidly. At the cannula entry site into the suprachoroidal space, a small patch of bare sclera was present that was devoid of choroidal vasculature. This was not associated with any retinal detachments or vitreous traction bands (by ophthalmic observation) with vehicle, palucorcel, or pUTC administration. No abnormalities were noted in the neighboring tissues.

Angiography

In four animals that received palucorcel, focal changes were observed on FA and ICG angiography in the area of subretinal delivery. No dye leakage was noted from either the retinal or choroidal vasculature. At the 1-month angiogram, one animal had focal areas of FA hyperfluorescence within the area corresponding to the surgically induced subretinal bleb. Two focal areas of hypofluorescence were visible on ICG angiograms in the same vicinity for that animal. On 3-month angiograms, focal areas of FA hypofluorescence and/or hyperfluorescence were present in the superior or superotemporal region of the fundus of two animals (both administered with palucorcel) in the area of the subretinal bleb. Focal hypofluorescent areas were present in the same locations on ICG angiograms and may indicate the subretinal injection site. In addition, tortuous small vessels were present at one hypofluorescent site for one of the two animals with focal hypofluorescence and/or hyperfluorescence on FA angiograms at month 3. Similar findings were observed in one animal administered with pUTC at months 1 and 3.

Electroretinography

No changes in scotopic or photopic ERG amplitudes and implicit times were observed in eyes that were administered with palucorcel or pUTC as compared with eyes treated with CS-SCO vehicle. At 1 month and 3 months post dose, minor increases or decreases in average amplitudes and implicit times were often observed in all treated eyes compared to their baseline measurements and were considered to be related to individual variability and/or anesthesia levels (Supplementary Table S2).

Histopathology

Histopathologic observations in animals euthanized on day 1, month 1 (day 30), and month 3 (day 92) are summarized in Table 3. At all time points, some microscopic changes attributable to the experimental procedures were observed. On histopathologic examination, animals that were euthanized immediately after surgery characteristically had a peripheral retinal detachment at the site of injection; focal discontinuity of the retina, choroid, and/or sclera; infiltration of the limbus by a mixed population of inflammatory cells; and subretinal, subchoroidal, and/or limbus hemorrhage. The retinal detachment observed immediately post dose was limited to a focal area in the mid to posterior retina and corresponded to the injection site and the retinal elevations observed in ophthalmic observation. In some cases, test item cells were noted in the subretinal space (Fig. 4). Changes in the eyes of all groups of animals euthanized 1 month post dose included inflammatory cell infiltration (choroid, sclera, and/or limbus); fibrosis of the

Table 3. Summary of Microscopic Eye Findings

Microscopic Eye Findings	Euthanized Day 1		Euthanized Month 1			Euthanized Month 3		
	Palucorcel, $n = 3$	pUTC, $n = 3$	Vehicle, $n = 3$	Palucorcel, $n = 3$	pUTC, $n = 3$	Vehicle, $n = 3$	Palucorcel, $n = 3$	pUTC $n = 3$
Hemorrhage	2	2	–	–	1	–	–	–
Retina detachment	3	2	–	–	–	–	–	–
Choroid discontinuity	–	2	–	–	–	1	–	–
Retina discontinuity	–	2	–	–	–	–	–	–
Sclera discontinuity	–	1	–	–	–	–	–	–
Mixed cell limbus infiltration	1	–	2	3	3	2	–	2
Mixed cell sclera infiltration	–	–	–	1	–	–	–	–
Mononuclear cell choroid infiltration	–	–	2	3	–	–	3	1
Mononuclear cell sclera infiltration	–	–	1	2	–	2	2	2
Mononuclear cell retina infiltration	–	–	–	–	–	–	1	
Mononuclear cell conjunctiva infiltration	–	–	–	–	–	–	1	–
Retina disorganization	–	–	1	3	2	–	3	1
Retina gliosis	–	–	–	1	–	–	–	–
Sclera fibrosis	–	–	–	–	1	–	–	–
Choroid fibrosis	–	–	–	–	–	–	–	1
Macrophage aggregation	–	–	1	–	–	1	–	–
Retina degeneration	–	–	–	–	–	1	1	–
Retina atrophy	–	–	–	–	–	2	1	2
Retina granuloma	–	–	–	–	–	–	2	–

sclera; pigmented macrophages in the vitreous chamber, choroid, and retina; and disorganization of the retina (mainly the outer nuclear and photoreceptor layers). By 3 months post dose, microscopic findings included inflammatory cell infiltration (retina, choroid, and/or sclera), choroid fibrosis or discontinuity, and disorganization (Fig. 5). Retinal degeneration or atrophy, following focal discontinuity of the retina, remained present. In two of three animals that received palucorcel (xenogeneic) and were euthanized at month 3 (day 92), small focal retinal granulomas were observed (Fig. 5A). No granulomas were observed in eyes that received pUTC (allogeneic) or vehicle (Fig. 5B).

Serum Antibody Titers

Subretinal administration of palucorcel in CS-SCO 4B/BSS to minipigs (xenogeneic setting) resulted in detectable levels of anti-hUTC IgG antibodies in two of six animals (Supplementary Table S3). One animal (necropsied on day 30) showed elevated anti-hUTC IgG levels at week 2 post dosing. The antibody response continued to persist at month 1. Another animal (necropsied on day 92) showed no change at month 1 and elevated anti-hUTC IgG levels at 2 months post dosing that dropped off at month 3 post dosing. In contrast, subretinal administration of pUTC to minipigs (allogeneic) resulted in no detectable levels of anti-pUTC antibodies (Supplementary Table S4).

Discussion

This study evaluated the safety, tolerability, and clinical response of a single, subretinal injection of palucorcel or pUTC through the suprachoroidal space, using a novel injection cannula. The technology and techniques used in this novel subretinal delivery procedure were developed with expert retinal surgeons who helped to create a procedure that builds off previously known skills and devices. Surgical steps,

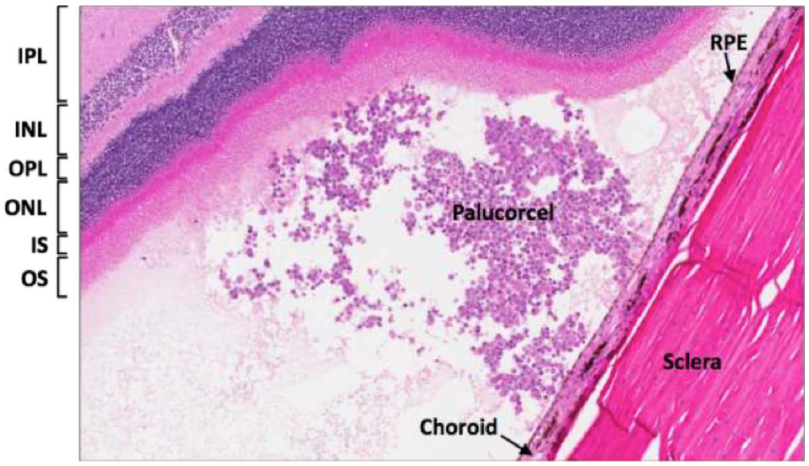

Figure 4. Palucorcel in the subretinal space with focal retinal detachment 1 day post surgery. IPL, inner plexiform layer; INL, inner nuclear layer; OPL, outer plexiform layer; ONL, outer nuclear layer; IS, inner segment; OS, outer segment.

Investigative Ophthalmology & Visual Science

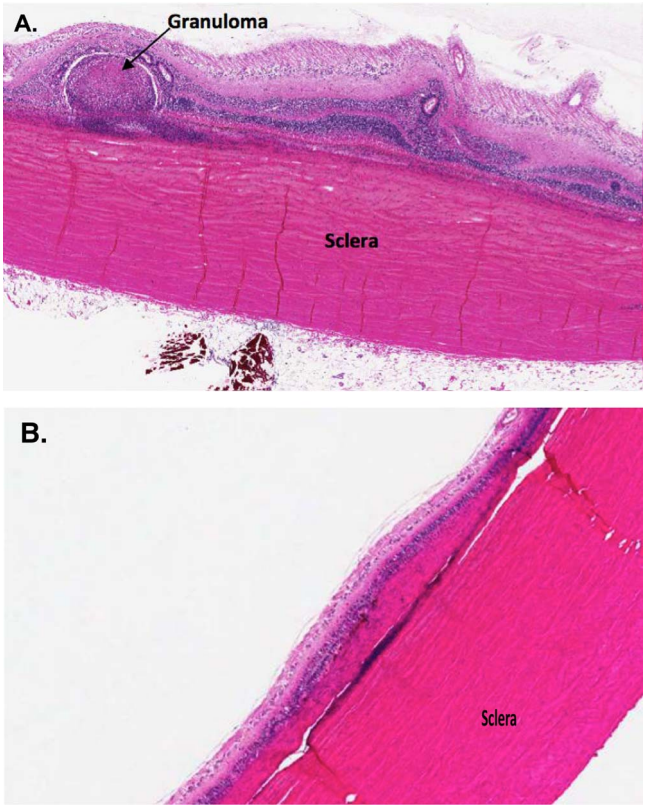

FIGURE 5. Retinal disorganization and granuloma (day 92) indicative of a xenogeneic response to palucorcel (**A**). Granulomas were not observed in the allogenic setting. Focal disorganization of the retina and minimal choroid fibrosis observed on day 92 in an animal that received pUTC (**B**).

such as conjunctival peritomy, eye rotation, choroidal exposure via a sclerotomy, and needle puncture of the choroid are all standard techniques used for decades in retinal detachment drainage procedures.[24] With regard to suprachoroidal cannulation, Olsen and colleagues[25] described a microcatheter for (1) insertion into the suprachoroidal space, (2) advancement to the macular region, and (3) delivery of a therapeutic product to the suprachoroidal space. El Rayes and Elborgy[26] used suprachoroidal cannulation to create an internal buckle for retinal detachments by injecting a long-lasting viscoelastic through an olive tip cannula. A number of subretinal injection procedures, particularly in the macular area, have made use of a transvitreal approach following a pars plana vitrectomy.[27–29] While many have used small-gauge nonextendible cannulas, some (including Komaromy and colleagues[30]) have proposed an extendable microneedle for improved subretinal injection. Nevertheless, subretinal delivery through a transvitreal approach remains challenging. Delivered product can escape out of the retinotomy into the vitreous during delivery, during needle withdrawal, or subsequently, as a stretched retina regains its original position. In addition, it is difficult to prevent expansion of the retinotomy during the delivery due to hand tremor. In the first in-human trial of palucorcel in patients with retinitis pigmentosa, the subretinal delivery of cells via a transretinal approach was associated with reflux and the formation of an epiretinal membrane in some patients.[23] Robotic-assisted surgical solutions may mitigate these challenges by providing high positional stability in all primary directions.[31,32] Positional stability also eliminates the need to proceed quickly with the injection, a requirement of manual procedures that may limit the applicability of any transvitreal injection technique in scarred retina. The association of robotics assistance with smart positioning devices or its combination with optical coherence tomography can further increase the precision of such deliveries in the future.

Reaching the subretinal space without breeching the integrity of the retina would obviate many of these concerns but requires suprachoroidal access to position the needle in the appropriate location, followed by advancement of the needle into the subretinal space.

Previous clinical and preclinical studies showed improvements in visual function when palucorcel was delivered subretinally.[17,18] While delivery of the cell product to the suprachoroidal space would be surgically easier, the subretinal space is an immune privilege site compared with all spaces beyond the RPE, which are not.[33] Cell survival would be decreased with delivery to the suprachoroidal space, and the possibility of retreatment if needed would be abrogated by the immune response. In addition, any trophic factors produced by the suprachoroidally placed cells, along with the cells themselves, would be rapidly cleared out of the eye through emissary channels[34,35] or would be hindered from reaching the retina by multiple barriers within the choroid, Bruch's membrane, and RPE.[36] For these reasons, the subretinal space was defined as the target for delivery, and the technique described here was developed to ensure the drug product is physically deposited adjacent to the target retinal cells.

In order to achieve our goal, a novel suprachoroidal positioning cannula coupled to a subretinal extension needle was required. The current procedure and device is novel in its ability to combine the positioning of a catheter in the suprachoroidal space with the safe delivery of a biologically active product to the subretinal space. In the process of developing the cannula/needle combination, several parameters were considered. These included the following: allowing the surgeon to safely position the catheter within the suprachoroidal space at a predetermined position (a rectangular design); the safe advancement of a microneedle to pierce through Bruch's membrane without damaging or perforating the retina (extension from the distal end of the catheter at an appropriate angle); and removing the effect of hand tremor and the need to proceed quickly with the injection.

Dose formulations were successfully administered into the subretinal space of Göttingen minipigs in 27 out of 27 eyes. CFSE fluorescently labeled cells or fluorescent vehicle were immediately visible post dose within the subretinal bleb, and no leakage of cells or vehicle into the vitreous was observed. Intraoperative observations generally indicated that the procedure was easy to perform and was associated with a relatively low rate of retinal perforations in comparison to the previous ab externo microcatheter-based system. The delivery blebs that were formed were closely observed. Most of the blebs remained fully formed when observed immediately after the procedure, with partial collapse observed in only 6 of 27 blebs. These collapses were typically present when the removal of the catheter was more complicated, for example, when the catheter was torqued during removal. These findings indicate that a smooth retraction along the same entry path is needed to prevent bleb collapse. The ophthalmic observation of retinal elevation in the area of the subretinal injection was observed and tracked over time, generally decreasing in severity from moderate at day 3 in some animals to slight or very slight by day 15, with resolution in all animals by 1 month (Supplementary Table S1). These intraoperative and ophthalmic exam findings provide supporting evidence for successful subretinal cell delivery followed by cell media fluid transport out of the subretinal space over time. This result on cell media fluid

transport is in agreement with previously described kinetics of macromolecules injected into the subretinal space.[37]

Histology performed immediately after dosing showed the presence of the expected retinal detachment. This histopathologic observation of retinal detachment corresponded to the ophthalmic observation of retinal elevations. In some eyes, cells could be observed in the subretinal space but not in the choroid or suprachoroidal space. At 3 months, in two of three eyes that received palucorcel (xenogeneic cells), histology revealed a focal granuloma. No such cell-mediated immune response was observed in animals administered with pUTC. A humoral immune response was also observed in animals receiving palucorcel. Detectable anti-hUTC IgG antibody levels were observed in two of six animals. Anti-hUTC was observed in one animal after 2 weeks, which persisted at 1 month when this animal was necropsied. Anti-hUTC was observed in a second animal at 2 months post dose. This animal was one of two animals observed with a focal granuloma. There were no detectable antibodies observed in animals receiving pUTC. For this study, in which human-derived cells were injected into minipigs, the observed mild immune response suggests a low likelihood for palucorcel to induce an immune reaction and is consistent with the low immune response to UTC observed in previous studies.[18,21]

This study provides data on the potential adverse events and other safety sequelae associated with this procedure for subretinal cell delivery via a suprachoroidal access. Data on procedure-related adverse events is generally lacking for other types of cells being evaluated as potential therapies for AMD. Preclinical studies of these products generally focus on the safety and tolerability of the cells, rather than the procedure[38,39]; furthermore, preclinical studies of subretinal cell delivery have reported the occurrence of retinal perforations and hemorrhages, though not generally the rates of these complications.[39–41] These findings highlight the need for a procedure and device with improved safety outcomes for subretinal delivery of therapeutic products.

Taken together, these results indicate that utilization of a suprachoroidal approach represents an improvement over previous surgical approaches, including ab externo and transvitreal routes of administration, for which rates of retinal detachments and retinal perforations were high and dependent on surgical expertise.[18,23] This approach appears to be less traumatic, having mitigated the risk of retinal detachment, retinal traction, and formation of vitreal membrane-like white opacity observed using previous methods of administration in the minipig eye, and may be more widely adaptable for a broad surgical audience.

The device and its procedure were the result of a large multidisciplinary team, with close interactions throughout the development process. Future efforts are focused on addressing the challenges of transferring this new technology to a wide range of surgeons, and studies assessing the safety and tolerability of this approach in patients with AMD are warranted.

Acknowledgments

The authors thank Clifford Sachs and Sicco Popma for their contributions. The authors alone are responsible for the content and writing of the paper.

Supported by Janssen Research & Development, LLC. Editorial assistance was provided by Megan Knagge of MedErgy, and was funded by Janssen Research & Development, LLC.

Disclosure: **M.D. de Smet**, Janssen Research & Development LLC (C, F); **J.L. Lynch**, Janssen Research & Development (E); **N.S. Dejneka**, Janssen Research & Development (E); **M. Keane**, Janssen Research & Development (E); **I.J. Khan**, Janssen Research & Development (E)

References

1. Girmens JF, Sahel JA, Marazova K. Dry age-related macular degeneration: a currently unmet clinical need. *Intractable Rare Dis Res*. 2012;1:103–114.
2. Grunwald JE, Daniel E, Huang J, et al. Risk of geographic atrophy in the comparison of age-related macular degeneration treatments trials. *Ophthalmology*. 2014;121:150–161.
3. Holz FG, Strauss EC, Schmitz-Valckenberg S, van Lookeren CM. Geographic atrophy: clinical features and potential therapeutic approaches. *Ophthalmology*. 2014;121:1079–1091.
4. Ambati J, Ambati BK, Yoo SH, Ianchulev S, Adamis AP. Age-related macular degeneration: etiology, pathogenesis, and therapeutic strategies. *Surv Ophthalmol*. 2003;48:257–293.
5. Algvere PV, Kvanta A, Seregard S. Drusen maculopathy: a risk factor for visual deterioration. *Acta Ophthalmol*. 2016;94:427–433.
6. Biesemeier A, Taubitz T, Julien S, Yoeruek E, Schraermeyer U. Choriocapillaris breakdown precedes retinal degeneration in age-related macular degeneration. *Neurobiol Aging*. 2014;35:2562–2573.
7. Zarubina AV, Neely DC, Clark ME, et al. Prevalence of subretinal drusenoid deposits in older persons with and without age-related macular degeneration, by multimodal imaging. *Ophthalmology*. 2016;123:1090–1100.
8. Beatty S, Koh H, Phil M, Henson D, Boulton M. The role of oxidative stress in the pathogenesis of age-related macular degeneration. *Surv Ophthalmol*. 2000;45:115–134.
9. Grassmann F, Fleckenstein M, Chew EY, et al. Clinical and genetic factors associated with progression of geographic atrophy lesions in age-related macular degeneration. *PLoS One*. 2015;10:e0126636.
10. Adrion C, Fleckenstein M, Schmitz-Valckenberg S, Holz F, Mansmann U. Estimation of disease onset for patients with geographic atrophy due to age-related macular degeneration. *Gesundheitswesen*. 2010;72:V207.
11. Balaratnasingam C, Messinger JD, Sloan KR, Yannuzzi LA, Freund KB, Curcio CA. Histologic and optical coherence tomographic correlates in drusenoid pigment epithelium detachment in age-related macular degeneration. *Ophthalmology*. 2017;124:644–656.
12. Klein R, Klein BE, Knudtson MD, Meuer SM, Swift M, Gangnon RE. Fifteen-year cumulative incidence of age-related macular degeneration: the Beaver Dam Eye Study. *Ophthalmology*. 2007;114:253–262.
13. Lindblad AS, Lloyd PC, Clemons TE, et al. Change in area of geographic atrophy in the Age-Related Eye Disease Study: AREDS report number 26. *Arch Ophthalmol*. 2009;127:1168–1174.
14. Chew EY, Clemons TE, Agron E, et al. Ten-year follow-up of age-related macular degeneration in the age-related eye disease study: AREDS report no. 36. *JAMA Ophthalmol*. 2014;132:272–277.
15. Singer M. Advances in the management of macular degeneration. *F1000Prime Rep*. 2014;6:29.
16. Biarnes M, Mones J, Alonso J, Arias L. Update on geographic atrophy in age-related macular degeneration. *Optom Vis Sci*. 2011;88:881–889.
17. Lund RD, Wang S, Lu B, et al. Cells isolated from umbilical cord tissue rescue photoreceptors and visual functions in a rodent model of retinal disease. *Stem Cells*. 2007;25:602–611.
18. Ho AC, Chang TS, Samuel M, Williamson P, Willenbucher RF, Malone T. Experience with a subretinal cell-based therapy in

patients with geographic atrophy secondary to age-related macular degeneration. *Am J Ophthalmol*. 2017;179:67–80.

19. Cao J, Murat C, An W, et al. Human umbilical tissue-derived cells rescue retinal pigment epithelium dysfunction in retinal degeneration. *Stem Cells*. 2016;34:367–379.
20. Koh S, Kim N, Yin HH, Harris IR, Dejneka NS, Eroglu C. Human umbilical tissue-derived cells promote synapse formation and neurite outgrowth via thrombospondin family proteins. *J Neurosci*. 2015;35:15649–15665.
21. Lutton BV, Cho PS, Hirsh EL, et al. Approaches to avoid immune responses induced by repeated subcutaneous injections of allogeneic umbilical cord tissue-derived cells. *Transplantation*. 201090:494–501.
22. Cho PS, Messina DJ, Hirsh EL, et al. Immunogenicity of umbilical cord tissue derived cells. *Blood*. 2008;111:430–438.
23. Spencer WA. Analysis of an epiretinal membrane that developed after subretinal delivery of a cell therapy product in a subject with retinitis pigmentosa. Paper presented at: 49th Annual Meeting of the Retina Society; September 14–17, 2016; San Diego, CA, USA.
24. Hilton GF, Grizzard WS, Avins LR, Heilbron DC. The drainage of subretinal fluid: a randomized controlled clinical trial. *Retina*. 1981;1:271–280.
25. Olsen TW, Feng X, Wabner K, et al. Cannulation of the suprachoroidal space: a novel drug delivery methodology to the posterior segment. *Am J Ophthalmol*. 2006;142:777–787.
26. El Rayes EN, Elborgy E. Suprachoroidal buckling: technique and indications. *J Ophthalmic Vis Res*. 2013;8:393–399.
27. Maguire AM, Simonelli F, Pierce EA, et al. Safety and efficacy of gene transfer for Leber's congenital amaurosis. *N Engl J Med*. 2008;358:2240–2248.
28. Olivier S, Chow DR, Packo KH, MacCumber MW, Awh CC. Subretinal recombinant tissue plasminogen activator injection and pneumatic displacement of thick submacular hemorrhage in age-related macular degeneration. *Ophthalmology*. 2004; 111:1201–1208.
29. Stout JT, Francis PJ. Surgical approaches to gene and stem cell therapy for retinal disease. *Hum Gene Ther*. 2011;22:531–535.
30. Komaromy AM, Varner SE, de Juan E, Acland GM, Aguirre GD. Application of a new subretinal injection device in the dog. *Cell Transplant*. 2006;15:511–519.
31. de Smet MD, Meenink TC, Janssens T, et al. Robotic-assisted cannulation of occluded retinal veins. *PLoS One*. 2016;11: e0162037.
32. Molaei A, Abedloo E, de Smet MD, et al. Toward the art of robotic-assisted vitreoretinal surgery. *J Ophthalmic Vis Res*. 2017;12:212–218.
33. Streilein JW. Ocular immune privilege: therapeutic opportunities from an experiment of nature. *Nat Rev Immunol*. 2003; 3:879–889.
34. Gilger BC, Abarca EM, Salmon JH, Patel S. Treatment of acute posterior uveitis in a porcine model by injection of triamcinolone acetonide into the suprachoroidal space using microneedles. *Invest Ophthalmol Vis Sci*. 2013;54:2483–2492.
35. Toris CB, Pederson JE. Effect of intraocular pressure on uveoscleral outflow following cyclodialysis in the monkey eye. *Invest Ophthalmol Vis Sci*. 1985;26:1745–1749.
36. Steinberg RH, Sheldon SM. Transport and membrane properties of the retinal pigment epithelium. In: Zinn KM, Marmor MF, eds. *The Reginal Pigment Epithelium*. Cambridge, MA: Harvard University Press; 1979:205–225.
37. Marmor MF, Negi A, Maurice DM. Kinetics of macromolecules injected into the subretinal space. *Exp Eye Res*. 1985;40:687–696.
38. Meyer CH, Holz FG. Preclinical aspects of anti-VEGF agents for the treatment of wet AMD: ranibizumab and bevacizumab. *Eye (Lond)*. 2011;25:661–672.
39. Rosa RH, Roddy GW, Krause UC, Prockop DJ. Feasibility study on intravitreal and subretinal delivery of adult stem/progenitor cells (MSCs) for retinal repair. *Invest Ophthalmol Vis Sci*. 2010;51:3153.
40. Jacobson SG, Boye SL, Aleman TS, et al. Safety in nonhuman primates of ocular AAV2-RPE65, a candidate treatment for blindness in Leber congenital amaurosis. *Hum Gene Ther*. 2006;17:845–858.
41. Nork TM, Murphy CJ, Kim CB, et al. Functional and anatomic consequences of subretinal dosing in the cynomolgus macaque. *Arch Ophthalmol*. 2012;130:65–75.

Investigative Ophthalmology & Visual Science